Heart and Vessels (2022) 37:1097–1105
https://doi.org/10.1007/s00380-021-02010-x

ORIGINAL ARTICLE

Healed neointima of in-stent restenosis lesions in patients with stable angina pectoris: an intracoronary optical coherence tomography study

Hideo Amano[1] · Yoshimasa Kojima[1] · Shojiro Hirano[1] · Yosuke Oka[1] · Hiroto Aikawa[1] · Shingo Matsumoto[1] · Ryota Noike[1] · Takayuki Yabe[1] · Ryo Okubo[1] · Takanori Ikeda[1]

Received: 18 September 2021 / Accepted: 3 December 2021 / Published online: 15 January 2022

Abstract
The phenomenon to heal neointimal rupture or thrombus after coronary stenting occurs as well as in native coronary artery. We investigated clinical characteristics and neointimal vulnerability of healed neointima by optical coherence tomography (OCT). We treated 67 lesions by percutaneous coronary intervention for in-stent restenosis (ISR) and conducted OCT examinations. Healed neointima was defined as neointima having one or more layers with different optical densities and a clear demarcation from underlying components. ISR with healed neointima was found in 49% (33/67) of the lesions. Compared to ISR without healed neointima, ISR with healed neointima showed significantly longer stent age (102 ± 72 vs. 31 ± 39 months, $P < 0.001$), lower frequency of dual antiplatelet therapy [42% (14/33) vs. 74% (25/34), $P = 0.017$], lower use of angiotensin-converting enzyme inhibitor or angiotensin II receptor blocker (ACE-I or ARB) [61% (20/33) vs. 91% (31/34), $P = 0.028$], lower usage of second-generation drug-eluting stents (DESs) [36% (12/33) vs. 63% (22/34), $P = 0.029$], higher usage of thick-strut stents [42% (14/33) vs. 15% (5/34), $P = 0.012$], larger neointimal area (6.8 ± 2.6 vs. 5.2 ± 1.8 mm^2, $P = 0.005$), higher incidence of thin-cap fibroatheroma [58% (19/33) vs. 21% (7/34), $P = 0.002$], neointimal rupture [45% (15/33) vs. 9% (3/34), $P = 0.001$], and lower incidence of stent underexpansion [15% (5/33) vs. 44% (15/34), $P = 0.010$]. In conclusions, ISR with healed neointima was associated with neointimal vulnerability, stent age, stent type, stent strut thickness, stent expansion, antiplatelet therapy, and use of ACE-I or ARB.

Keywords Healed neointima · Optical coherence tomography · In-stent restenosis

Introduction

Healed plaques in native coronary artery indicate the repair phenomenon of ruptured fibrous caps and erosions in pathology studies [1–3]. Healed plaques associated with plaque vulnerability on optical coherence tomography (OCT), local and systemic inflammation, and coronary risk factors in acute coronary syndrome lesions (ACS) [4].

The development of atherosclerosis within neointimal tissue after coronary stenting, called neoatherosclerosis, has been reported in a pathologic study [5]. Neoatherosclerosis detected by OCT after stent implantation is associated with stent thrombosis and target lesion revascularization [6, 7].

A similar phenomenon of healed plaque in native coronary plaque is considered to occur in neointima after stent implantation [8]. However, there are few reports in the literature regarding clinical characteristics and neointimal vulnerability of healed tissue in neointima, which is called healed neointima in this study.

OCT has high resolution [9], and it is the only modality able to detect neointimal characteristics [10, 11]. We investigated the clinical, procedure, and neointimal characteristics of healed neointima in in-stent restenosis (ISR) lesions by OCT.

Clarifying the factors that cause healed neointima is important for avoiding stent restenosis and stent thrombosis, and might enable clinicians to improve procedural strategies and medical therapy.

✉ Hideo Amano
amanohide@med.toho-u.ac.jp

[1] Department of Cardiovascular Medicine, Toho University Faculty of Medicine, 6-11-1 Omorinishi, Ota-ku, Tokyo 143-8541, Japan

Methods

Patient population

Between February 2012 and July 2021, we performed percutaneous coronary intervention (PCI) for 477 lesions for ISR at Toho University Faculty of Medicine. The present study consecutively enrolled 87 lesions treated by PCI for ISR that underwent OCT examinations before PCI. The exclusion criteria were as follows: (1) left main trunk disease, (2) chronic total occlusion, (3) cardiogenic shock, (4) tortuous or calcified vessels with expected difficulty in advancing the OCT catheter, (5) large vessel expected limitation in OCT imaging, (6) the presence of large amounts of thrombus, (7) congestive heart failure with left ventricular ejection fraction < 40%, and (8) renal insufficiency with baseline serum creatinine > 2.0 mg/dL. This study was approved by the Toho University Omori Medical Center Ethics Committee (approval number M20107). In this observational study, comprehensive agreement was obtained from all patients in the opt-out form on the website of Toho University Omori Medical Center.

Stable angina pectoris (SAP) was defined as chest pain on exertion without changes in frequency or intensity for at least 4 weeks, and the patients had myocardial ischemia based on either stress myocardial scintigraphy or fractional flow reserve. The estimated glomerular filtration rate was calculated using the Chronic Kidney Disease Epidemiology Collaboration equation [12]. Chronic kidney disease was defined as a patient having an estimated glomerular filtration rate of < 60 mL/min/1.73 m^2, which is consistent with the National Kidney Foundation classification stages 3–5 [13].

The treatment strategy and the selection of stents at the time of baseline PCI were determined by the physicians. PCI was performed by the conventional strategy using OCT. Dual antiplatelet therapy was recommended for patients with bare metal stents (BMSs) for ≥ 2 months, and for patients with drug-eluting stents (DESs) for ≥ 6 months after stent implantation.

Antithrombotic treatment regimens at ISR were defined as follows: (1) single antiplatelet therapy: aspirin or $P2Y_{12}$ inhibitor; (2) dual antiplatelet therapy: aspirin and $P2Y_{12}$ inhibitor; (3) dual antithrombotic therapy: oral anticoagulation (OAC) plus aspirin or $P2Y_{12}$ inhibitor; (4) triple antithrombotic therapy OAC plus aspirin and $P2Y_{12}$ inhibitor; (5) Anticoagulant monotherapy: warfarin or direct oral anticoagulants.

First-generation DESs were defined as the first-generation sirolimus-eluting stent: Cypher, or paclitaxel-eluting stent paclitaxel-eluting stents: TAXUS; second-generation DESs were defined as the DESs that became available after the first-generation DESs.

ISR was defined as ≥ 50% diameter stenosis at the stented site. Stents with a strut thickness < 100 μm were classified as thin, whereas stents with a strut thickness ≥ 100 μm were classified as thick [14].

PCI procedure

At the time of PCI for ISR, all patients received aspirin (100 mg/day), clopidogrel (75 mg/day), or prasugrel (3.75 mg/day approved daily dose in Japan) before PCI. Intravenous heparin (100 U/kg) and intracoronary nitrates were administered at the beginning of the procedure. After initial angiography, OCT was performed. Thrombolysis In Myocardial Infarction (TIMI) flow grade was assessed as described previously [15]. The angiographic slow flow was defined as a decrease of at least 1 grade in TIMI flow during PCI or final TIMI flow grade 0 and 1 or 2, with no evidence of thrombus, spasm, or dissection. Periprocedural myocardial Infarction was defined as a creatine kinase-myocardial band (CK-MB) elevation > 3 × the upper limit of normal within 24 h post-PCI. Platelet glycoprotein IIb/IIIa receptor inhibitors were not used because these are not available in Japan.

OCT procedure and analysis

OCT was performed with a frequency-domain (C7-XR, OCT Intravascular Imaging System; St Jude Medical, St Paul, MN, USA) OCT system. Before PCI, a 2.7 F OCT imaging catheter (Dragonfly; St Jude Medical) was advanced distal to the end of the stent, and automated pullback was performed with blood clearance by the injection of contrast medium or dextran. The OCT data were stored digitally and analyzed by an ILUMIEN OCT imaging system (St Jude Medical). Offline analyses were performed by two experienced observers blinded to the patients' clinical data. Any discrepancies between the observers were resolved by consensus. Morphologic evaluation of OCT images was performed from the distal to proximal edge of the stent.

Lipid-laden neointima was defined as a diffusely bordered signal-poor region with rapid signal attenuation [16]. Of lipid-laden neointima, thin-cap fibroatheromas (TCFAs) were defined as a fibrous cap thickness ≤ 65 μm at the thinnest part [16]. Neointimal rupture was a break in the fibrous cap that connected the lumen with the underlying lipid pool [17]. Calcification inside the neointima was defined as a clearly delineated, signal-poor region with low backscatter [16]. Thrombus was defined as a mass attached to a luminal surface or floating within the lumen [16]. Microvessels were defined as a small vesicular or tubular structure with a diameter ≥ 50 μm and ≤ 300 μm [18]. Neoatherosclerosis was defined as lesions with lipid-laden neointima or calcification within neointima [19]. Healed neointima was defined

as neointima with one or more layers with different optical densities and a clear demarcation from underlying components on OCT (Fig. 1), as proposed in previous ex vivo and OCT studies [1, 20] and a recent histology validation study of native coronary tissue [4, 21].

For quantitative evaluation, all cross-sectional OCT images were evaluated and the following parameters were analyzed: the minimum lumen cross-sectional areas (CSA), minimum reference CSA, maximum neointimal hyperplasia CSA, maximum neointimal thickness, and proximal and distal reference lumen CSA. Mean reference CSA was the average of the proximal and distal reference lumen CSA. Proximal and distal reference lumen CSAs were at the slices with the largest lumen CSA within 5 mm proximal and distal to the stent edges. Stent expansion index was a ratio of minimal stent CSA to mean reference CSA. Stent underexpansion was MSA < 4.5 mm^2 and stent expansion index < 0.7 [22].

Statistical analysis

Statistical analysis was performed using SPSS version 24.0 (SPSS, Inc., Chicago, IL, USA). Continuous data were expressed as the mean ± SD. Categorical data are presented as numbers (percentages). Normality of the data was verified by the Kolmogorov–Smirnov test. Continuous data were compared using unpaired Student's t-test for normally distributed values or Mann–Whitney *U* test for nonnormally distributed values. Categorical variables were compared with the chi-square test or Fisher's exact test. *P* values of < 0.05 were considered statistically significant.

Results

We excluded cases as follows: (1) acute myocardial infarction or acute coronary syndrome ($n = 3$), (2) OCT examinations after ballooning ($n = 9$); and (3) poor OCT images ($n = 8$). Finally, we analyzed 67 SAP patients and 67 lesions that underwent OCT examinations before PCI. Lesions with healed neointima were found in 49% (33/67). The patients were divided into lesions with healed neointima ($n = 33$) and those without healed neointima ($n = 34$).

The clinical and procedure characteristics at the time of ISR are listed in Tables 1 and 2. Patients with healed neointima were significantly longer stent age (102 ± 72 vs. 31 ± 39 months, $P < 0.001$), showed significantly lower high-density lipoprotein cholesterol (HDL-C) at ISR (42 ± 12 vs. 53 ± 16 mg/dl, $P = 0.005$), higher triglycerides at ISR (178 ± 84 vs. 138 ± 67 mg/dl, $P = 0.039$), lower use of angiotensin-converting enzyme inhibitor or angiotensin II receptor blocker (ACE-I or ARB) [61% (20/33) vs. 91% (31/34), $P = 0.028$], lower frequency of dual antiplatelet therapy [42% (14/33) vs. 74% (25/34), $P = 0.017$], lower use of $P2Y_{12}$ inhibitor [55% (18/33) vs. 85% (29/34), $P = 0.006$], longer duration of antiplatelet therapy (74 ± 65 months vs. 19 ± 23 months, $P < 0.001$). The clinical and procedure characteristics at baseline are listed in Table 3. Compared to lesions without healed neointima, those with healed neointima had significantly lower use of second-generation DESs [36% (12/33) vs. 65% (22/34), $P = 0.029$], and higher use of thick-strut stents [42% (14/33) vs. 15% (5/34), $P = 0.012$]. There were no relations between with healed neointima and slow flow during PCI or procedural myocardial infarction. OCT findings at the time of ISR are listed in Table 4 and Fig. 2. Compared to lesions without healed neointima, those with healed neointima showed significantly larger mean reference CSA (9.2 ± 1.2 vs. 7.2 ± 2.0 mm^2, $P = 0.015$), larger neointimal hyperplasia CSA (6.8 ± 2.6 vs. 5.2 ± 1.8 mm^2, $P = 0.005$), higher neointima thickness (1.2 ± 0.3 vs. 0.9 ± 0.3 mm, $P < 0.001$), higher expansion index (0.88 ± 0.09 vs. 0.81 ± 0.18, $P = 0.043$), higher incidence of lipid-laden neointima [70% (23/33) vs. 32%

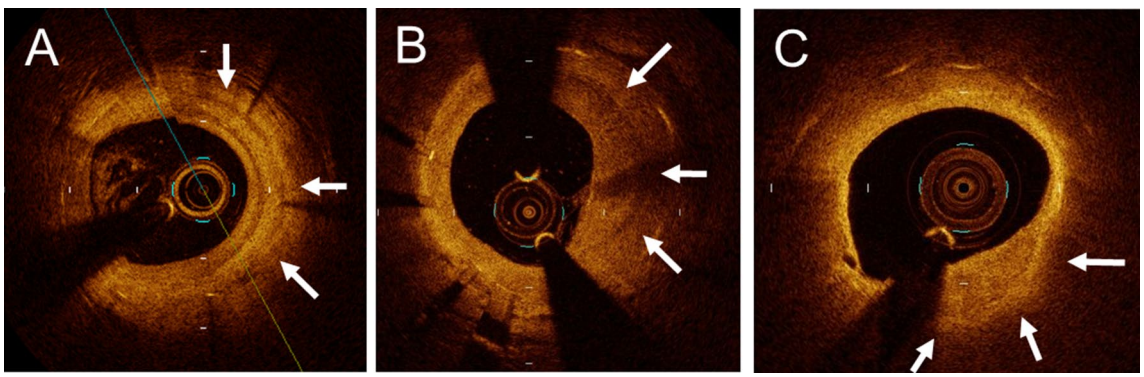

Fig. 1 Representative optical coherence tomography images of healed neointima Optical coherence tomography images of healed neointima (white arrow) (**A**–**C**)

Table 1 Clinical characteristics at the time of in-stent restenosis

Variable	Healed neointima		*P* value
	Yes ($n=33$)	Yes ($n=33$)	
Time since stent implantation (months)	102 ± 72	31 ± 39	< 0.001
Age (years)	68 ± 11	64 ± 11	0.171
Gender (male/female)	30/3	28/6	0.253
BMI (kg/m^2)	25 ± 3	24 ± 3	0.090
Hypertension	24 (73%)	24 (71%)	0.846
Diabetes mellitus	18 (55%)	12 (35%)	0.113
Dyslipidemia	29 (88%)	29 (85%)	0.520
Chronic kidney disease	11 (33%)	15 (44%)	0.365
Current smokers	14 (42%)	14 (41%)	0.918
Prior myocardial infarction	15 (45%)	18 (53%)	0.540
Prior coronary bypass	0 (0%)	1 (3%)	0.507
Family history of coronary artery disease	4 (12%)	5 (15%)	0.520
Clinical presentation of stable angina pectoris	33 (100%)	34 (100%)	–
Alb (g/dL)	4.1 ± 0.3	4.1 ± 0.4	0.438
Total cholesterol (mg/dl)	159 ± 35	170 ± 46	0.270
Low-density lipoprotein cholesterol (mg/dl)	86 ± 29	91 ± 41	0.594
High-density lipoprotein cholesterol (mg/dl)	42 ± 12	53 ± 16	0.005
Triglycerides (mg/dl)	178 ± 84	138 ± 67	0.039
Baseline creatine kinase (IU/L)	97 ± 68	103 ± 66	0.706
Post creatine kinase (IU/L)	120 ± 114	94 ± 71	0.264
Baseline creatine kinase-myocardial band (IU/L)	10 ± 5	9 ± 3	0.857
Post creatine kinase-myocardial band (IU/L)	13 ± 11	11 ± 7	0.276
Hemoglobin A1c (%)	6.6 ± 1.3	6.4 ± 0.9	0.517
Estimated glomerular filtration rate (mL/min/1.73 m^2)	58.4 ± 24.8	59.9 ± 0.2	0.824
Ejection fraction (%)	59.4 ± 12.0	60.4 ± 14.6	0.750
Medications in use			
Angiotensin-converting enzyme inhibitor or angiotensin II receptor blocker	20 (61%)	31 (91%)	0.003
Beta-blocker	19 (58%)	25 (74%)	0.169
Statin	26 (79%)	29 (85%)	0.487
Antithrombotic therapy			
Single antiplatelet therapy	14 (42%)	3 (9%)	0.017
Dual antiplatelet therapy	14 (42%)	25 (74%)	
Dual antithrombotic therapy	2 (6%)	1 (3%)	
Triple antithrombotic therapy	2 (6%)	3 (9%)	
Anticoagulant monotherapy	1 (3%)	0 (0%)	
Regimen of antiplatelet drug			
Aspirin	30 (91%)	32 (94%)	0.486
$P2Y_{12}$ inhibitor	18 (55%)	29 (85%)	0.006
Duration of antiplatelet therapy (Months)	74 ± 65	19 ± 23	< 0.001
Anticoagulant drug	5 (15%)	4 (12%)	0.734

(11/34), P = 0.002], TCFAs [58% (19/33) vs. 21% (7/34), $P = 0.002$], neointimal rupture [45% (15/33) vs. 9% (3/34), $P = 0.001$], thrombus [36% (12/33) vs. 3% (1/34), $P = 0.001$], macrophage accumulation [70% (23/33) vs. 15% (5/34), $P < 0.001$], microvessels [73% (24/33) vs. 32% (11/34), $P = 0.001$], neoatherosclerosis [76% (25/33) vs. 38% (13/34), $P = 0.002$], and lower incidence of stent underexpansion [15% (5/33) vs. 44% (15/34), $P = 0.010$]. The representative OCT images in 3 cases with or without healed neointima are demonstrated in Fig. 3.

Table 2 Procedure characteristics at the time of in-stent restenosis

Variable	Healed neointima		*P* value
	Yes ($n=33$)	No ($n=34$)	
Target vessel			
Left anterior descending coronary artery	20 (61%)	15 (44%)	0.401
Left circumflex coronary artery	4 (12%)	6 (18%)	
Right coronary artery	9 (27%)	13 (38%)	
Stent fracture	3 (9%)	4 (12%)	0.517
Reference vessel diameter (mm)	2.93 ± 0.55	2.84 ± 0.48	0.487
Minimal luminal diameter (mm)	0.91 ± 0.33	0.96 ± 0.35	0.512
Diameter stenosis (%)	69 ± 9	64 ± 15	0.129
Post reference vessel diameter (mm)	2.85 ± 0.54	3.15 ± 1.29	0.221
Post minimal luminal diameter (mm)	2.59 ± 0.51	2.61 ± 0.54	0.939
Post diameter stenosis (%)	8.4 ± 12.9	9.9 ± 15.9	0.677
Strategy for in-stent restenosis			
Drug-eluting stent	17 (52%)	16 (47%)	0.461
Paclitaxel-coated balloon	13 (39%)	17 (50%)	
Plain old balloon dilatation	3 (9%)	1 (3%)	
Slow flow during percutaneous coronary intervention	3 (9%)	4 (12%)	0.721
Procedural myocardial infarction	1 (3%)	0 (0%)	0.493

Table 3 Clinical and procedure characteristics at baseline

Variable	Healed neointima		*P* value
	Yes ($n=33$)	No ($n=34$)	
Age (years)	60 ± 11	61 ± 10	0.494
Clinical presentation			
Acute coronary syndrome	9 (27%)	12 (35%)	0.479
Stable angina pectoris	24 (73%)	22 (65%)	
Medications in use			
Angiotensin-converting enzyme inhibitor or angiotensin II receptor blocker	13 (39%)	19 (56%)	0.275
Beta-blocker	9 (27%)	10 (29%)	0.846
Statin	15 (45%)	13 (38%)	0.549
Stent type			
Bare metal stent	15 (45%)	11 (32%)	0.029
First-generation drug-eluting stent	6 (18%)	1 (3%)	
Second-generation drug-eluting stent	12 (36%)	22 (65%)	
Stent strut thickness			
Thin strut < 100 μm	19 (58%)	29 (85%)	0.012
Thick-strut > 100 μm	14 (42%)	5 (15%)	
Stent			
Stent diameter (mm)	3.23 ± 0.54	2.98 ± 0.43	0.052
Total stent length (mm)	34.6 ± 22.7	36.4 ± 20.1	0.750
Overlap stenting	14 (42%)	16 (47%)	0.703
Calcification on angiography	10 (30%)	11 (32%)	0.856

Discussion

This is the first study to investigate the characteristics and significance of healed neointima on OCT. The main findings of this study are as follows: (1) patients with healed neointima were associated with lower HDL-C, higher triglycerides, and lower use of ACE-I or ARB, lower frequency of dual antiplatelet therapy, and lower use of $P2Y_{12}$ inhibitor; (2) lesions with healed neointima showed longer stent age, lower usage of second-generation DESs, and higher usage of thick-strut stents; (3) lesions with healed neointima showed higher vulnerability; (4) lesions with healed neointima showed larger stent area, larger neointima area, higher neointima thickness, and lower stent underexpansion.

Relationship between healed neointima and neointimal characteristics

In our study, lesions with healed neointima showed a higher incidence of lipid-laden neointima, TCFA-like neointima, neointimal rupture, macrophage accumulation, thrombus and microvessels, so healed neointima was associated with high vulnerability. Healed plaques in native coronary artery indicate the repair phenomenon of ruptured fibrous caps [1, 2]. Smooth muscle cells, proteoglycans and type III collagen infiltrated into an organizing thrombus after rupturing the fibrous cap. Type III collagen is replaced by type I collagen. Repeated healing plaques formed multiple layers, increased the plaque burden, and then narrowed the lumen. Healed plaques are associated with plaque vulnerability on OCT,

Table 4 Optical coherence tomography findings

Variable	Healed neointima		*P* value
	Yes ($n=33$)	No ($n=34$)	
Minimum lumen cross-sectional area (mm^2)	1.7 ± 0.8	1.8 ± 1.2	0.441
Minimum stent cross-sectional area (mm^2)	7.5 ± 2.7	5.8 ± 2.3	0.007
Mean reference cross-sectional area (mm^2)	9.2 ± 1.2	7.2 ± 2.0	0.015
Maximum neointimal hyperplasia cross-sectional area (mm^2)	6.8 ± 2.6	5.2 ± 1.8	0.005
Maximum neointimal thickness (mm)	1.2 ± 0.3	0.9 ± 0.3	< 0.001
Expansion index	0.88 ± 0.09	0.81 ± 0.18	0.043
Stent underexpansion	5 (15%)	15 (44%)	0.010

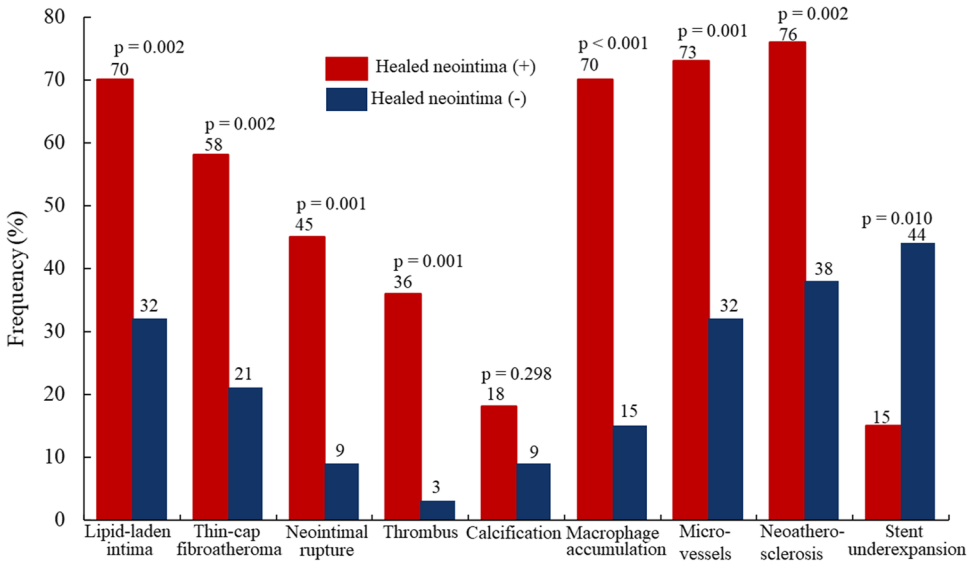

Fig. 2 Comparison of neointimal characteristics in optical coherence tomography according to the presence and absence of healed neointima. Lesions with healed neointima showed significantly higher incidence of lipid-laden neointima, thin-cap fibroatheromas, neointimal rupture, thrombus, macrophage accumulation, microvessels and lower incidence of stent underexpansion than those without healed neointima

local and systemic inflammation, coronary risk factors, and severe stenosis in ACS lesions [4]. Even in SAP patients, healed plaques are associated with features of plaque vulnerability and advanced atherosclerosis [23].

A similar phenomenon of healed plaque in native coronary artery is considered to occur in ISR lesions [8]. The overlying thrombus due to neointimal rupture will heal with inflammation, smooth muscle cell infiltration, and deposition of proteoglycans and collagen matrix, resulting in intraluminal stenosis and in-stent restenosis [8]. In addition, it is considered that other mechanism of healed neointima is irregular plaque protrusion or thrombus. An OCT study reports that irregular protrusion was associated with thrombus previous stent implantation [24]. Therefore, healed neointima was associated with high vulnerability of neoimtima. Healed neointima is not included in definition of neoatherosclerosis on OCT: therefore, healed neointima is worth investigating as a figure of neointimal vulnerability. Pathologic and OCT studies have reported that neoatherosclerosis is associated with late stent failure [19, 25, 26]. In addition, pathological studies reports that the accumulation of small rupture healings leads to plaque growth and lumen narrowing in native coronary [2, 27]. It needs longer times to heal multiple small ruptures, thrombi, or erosions in neointima, so the stent age in lesions with healed neointima was longer and the neointima volume was larger than those without healed neointima.

Relationship between healed neointima and procedure characteristics

Lesions with healed neointima were more prevalent in first-generation DESs, and less prevalent in second-generation generation DESs in our study. An OCT study reported that neoatherosclerosis with a short duration after stent implantation in second-generation DESs is less frequent than that in first-generation DESs [28]. In previous studies, second-generation DESs had greater strut coverage with less inflammation and less fibrin deposition [29], those effect might be protective by healing neointima.

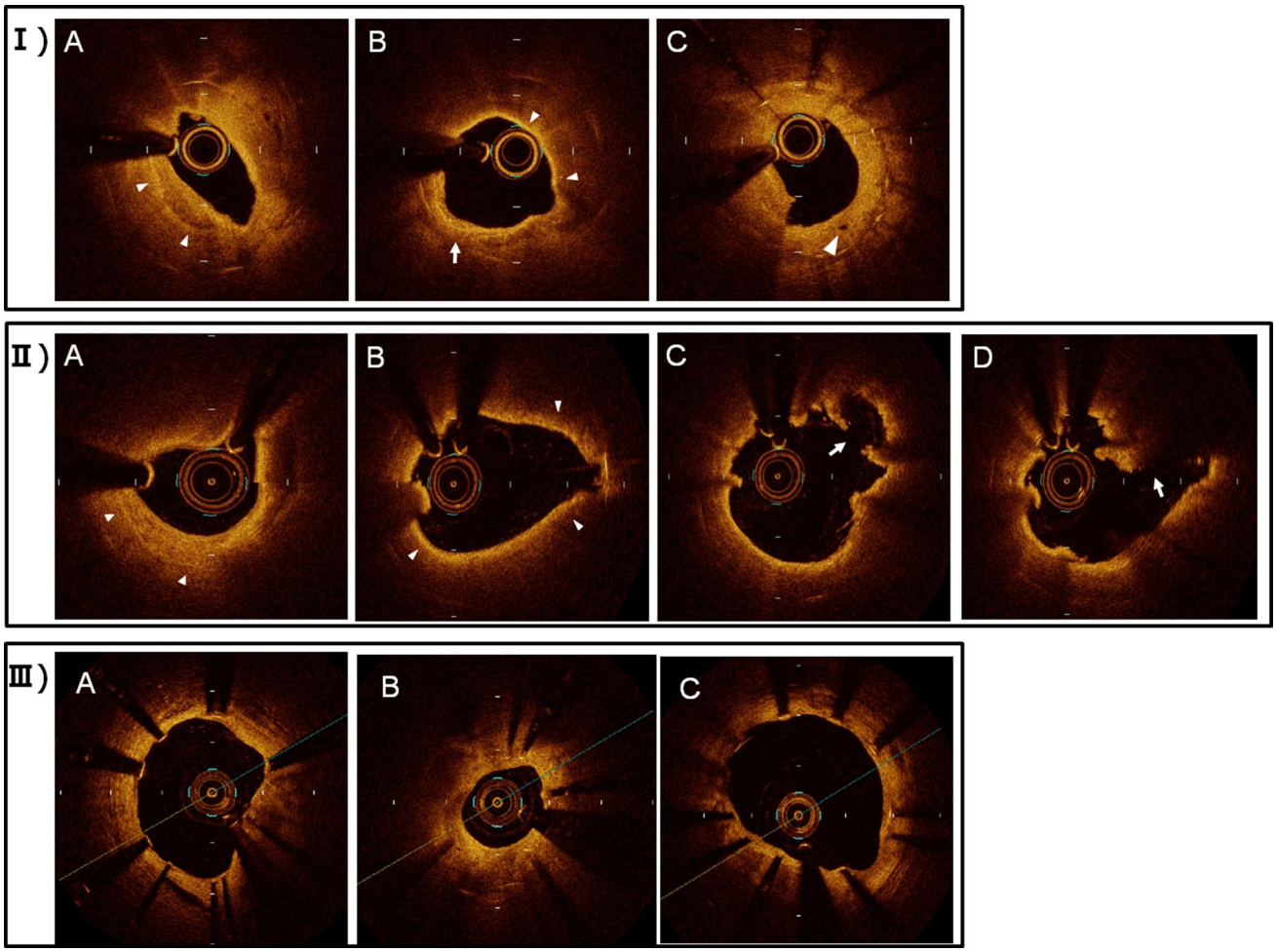

Fig. 3 Representative optical coherence tomography images of in-stent restenosis with or without healed neointima. **I** In-stent restenosis with healed neointima in the left anterior descending coronary artery (**A**–**C**). **A** Healed neointima was located at the 6–9 o'clock position (white arrowhead). **B** Thin-cap fibroatheroma-like neointima was located at the 11–4 o'clock position (white arrowhead). Macrophage accumulation was located at the 6–9 o'clock position (white arrow). **C** Microvessels were located at the 5 o'clock position (white arrowhead). **II** In-stent restenosis with healed neointima in the left anterior descending coronary artery (**A**–**D**). **A** Healed neointima was located at the 6–9 o'clock position (white arrowhead). **B** Thin-cap fibroatheroma-like neointima was circumferentially located (white arrowhead). **C** The lesion had a neointimal rupture (white arrow). **D** The thrombus was located at the 1–3 o'clock position (white arrow). **III** In-stent restenosis without healed neointima in the right coronary artery (**A**–**C**). **B** Optical coherence tomography images showed stent restenosis with stent underexpansion in the midportion of the stent segment. The lesion had not healed neointima. The lesion showed a small neointimal area

In our study, lesions with healed neointima were more prevalent in thick-strut stents. Kitabata et al. reported that lipid-laden intima, thin-cap fibroatheroma–like intima, and intimal disruption were more frequently observed in the thick-strut stents group than in the thin-strut stents group [14]. Thick-strut stents were associated with neointima vulnerability, including healed neointima.

Relationship between healed neointima and clinical characteristics

Patients with healed neointima were associated with lower HDL-C, lower use of ACE-I or ARB, lower frequency of dual antiplatelet therapy, and lower use of $P2Y_{12}$ inhibitor at the time of ISR. High antioxidant and anti-inflammatory activities of HDL-C protect against atherosclerosis [30, 31]. A previous study reported that impaired HDL-C function was associated with neoatherosclerosis and future stent failure [32]. It has been reported that the absence of ACE-I or ARB was associated with neoatherosclerosis [19, 28]. ACE-I prevents in-stent restenosis by stimulating apoptosis [33]. HDL-C and triglycerides control with medical therapy, and the use of ACE-I or ARB might prevent the development of healed neointima. Lower frequency of dual antiplatelet therapy and lower use of $P2Y_{12}$ inhibitor may have affected thrombus formation following

small ruptures, which is one of the mechanisms of healed neointima.

Relationship between healed neointima and stent expansion

Lesions without healed neointima showed a higher incidence of stent underexpansion. Stent underexpansion causes sparse and crowding distribution of each stent strut, and then leads to stent restenosis [34]. The main factor of stent restenosis in-stent underexpansion is mechanical radial stress [35], hence, the speed from stent implantation to in-stent restenosis was early, and the neointimal volume in-stent underexpansion was small. Therefore, lesions without healed neointima showed shorter stent age and smaller neointimal area in our study. In a previous study, second-generation DESs in OCT-detected ISR with neoatherosclerosis had a smaller stent area, stent fracture or deformation, and shorter stent age than first-generation DESs or BMSs [28]. High-frequency usage of second-generation DESs in ISR without healed neointima might be associated with stent underexpansion, smaller stent areas, and shorter stent ages.

Clinical implications

As clinical implications, healed neointima is one of the indicators of neointima vulnerability on OCT. The ISR mechanism differed between lesions with healed neointima and those without; therefore, detecting of healed neointima on OCT is useful for clarifying the ISR mechanism and making treatment strategies of ISR lesion. Medical therapy and stent selection are needed to avoid ISR with healed neointima, and larger dilatation of the lesions at baseline PCI might be needed to avoid ISR without healed neointima.

Limitations

There are several limitations of our analysis. This was a retrospective and single-center study on a limited number of patients who could undergo OCT studies. The treatment strategy and the selection of stent type at the time of baseline PCI were at the discretion of the physician. OCT light sources are attenuated behind lipid-laden neointima; therefore, the presence of healed neointima behind lipid-laden neointima might be underestimated.

Conclusions

ISR with healed neointima was associated with neointimal vulnerability, stent age, stent type, stent strut thickness, stent expansion, antiplatelet therapy, HDL-C and triglycerides levels, and use of ACE-I or ARB.

Declarations

Conflict of interest The authors do not have any potential conflicts of interest associated with this paper.

References

1. Otsuka F, Joner M, Prati F, Virmani R, Narula J (2014) Clinical classification of plaque morphology in coronary disease. Nat Rev Cardiol 11:379–389
2. Burke AP, Kolodgie FD, Farb A, Weber DK, Malcom GT, Smialek J, Virmani R (2001) Healed plaque ruptures and sudden coronary death: evidence that subclinical rupture has a role in plaque progression. Circulation 103:934–940
3. Virmani R, Kolodgie FD, Burke AP, Farb A, Schwartz SM (2000) Lessons from sudden coronary death: a comprehensive morphological classification scheme for atherosclerotic lesions. Arterioscler Thromb Vasc Biol 20(5):1262–1275
4. Fracassi F, Crea F, Sugiyama T, Yamamoto E, Uemura S, Vergallo R, Porto I, Lee H, Fujimoto J, Fuster V, Jang IK (2019) Healed culprit plaques in patients with acute coronary syndromes. J Am Coll Cardiol 73:2253–2263
5. Nakazawa G, Otsuka F, Nakano M, Vorpahl M, Yazdani SK, Ladich E, Kolodgie FD, Finn AV, Virmani R (2011) The pathology of neoatherosclerosis in human coronary implants bare-metal and drug-eluting stents. J Am Coll Cardiol 57:1314–1322
6. Kang SJ, Mintz GS, Akasaka T, Park DW, Lee JY, Kim WJ, Lee SW, Kim YH, Whan Lee C, Park SW, Park SJ (2011) Optical coherence tomographic analysis of in-stent neoatherosclerosis after drug-eluting stent implantation. Circulation 123:2954–2963
7. Amabile N, Souteyrand G, Ghostine S, Combaret N, Slama MS, Barber-Chamoux N, Motreff P, Caussin C (2014) Very late stent thrombosis related to incomplete neointimal coverage or neoatherosclerotic plaque rupture identified by optical coherence tomography imaging. Eur Heart J Cardiovasc Imaging 15:24–31
8. Otsuka F, Byrne RA, Yahagi K, Mori H, Ladich E, Fowler DR, Kutys R, Xhepa E, Kastrati A, Virmani R, Joner M (2015) Neoatherosclerosis: overview of histopathologic findings and implications for intravascular imaging assessment. Eur Heart J 36:2147–2159
9. Huang D, Swanson EA, Lin CP, Schuman JS, Stinson WG, Chang W, Hee MR, Flotte T, Gregory K, Puliafito CA (1991) Optical coherence tomography. Science 254:1178–1181
10. Yamamoto W, Fujii K, Otsuji S, Takiuchi S, Kakishita M, Ibuki M, Hasegawa K, Ishibuchi K, Tamaru H, Yasuda S, Ishii R, Nakabayashi S, Kusumoto H, Higashino Y (2020) Optical coherence tomography characteristics of in-stent restenosis after drug-eluting stent implantation: a novel classification and its clinical significance. Heart Vessels 35:38–45
11. Oka N, Kadohira T, Fujii K, Kitahara H, Fujimoto Y, Kobayashi Y (2019) Microbubble contrast enhancement of neointima after drug-eluting stent implantation: an optical coherence tomography study. Heart Vessels 34:393–400
12. Levey AS, Bosch JP, Lewis JB, Greene T, Rogers N, Roth D (1999) A more accurate method to estimate glomerular filtration rate from serum creatinine: a new prediction equation. Modification of Diet in Renal Disease Study Group. Ann Intern Med 130:461–470
13. National Kidney Foundation (2002) K/DOQI clinical practice guidelines for chronic kidney disease: evaluation, classification, and stratification. Am J Kidney Dis 39:S1–S266
14. Kitabata H, Kubo T, Komukai K, Ishibashi K, Tanimoto T, Ino Y, Takarada S, Ozaki Y, Kashiwagi M, Orii M, Shiono Y,

Shimamura K, Hirata K, Tanaka A, Kimura K, Mizukoshi M, Imanishi T, Akasaka T (2012) Effect of strut thickness on neointimal atherosclerotic change over an extended follow-up period (≥ 4 years) after bare-metal stent implantation: intracoronary optical coherence tomography examination. Am Heart J 163:608–616
15. The TIMI Study Group (1985) The thrombolysis in myocardial infarction (TIMI) trial. Phase I findings. N Engl J Med 312:932–936
16. Tearney GJ, Regar E, Akasaka T, Adriaenssens T, Barlis P, Bezerra HG, Bouma B, Bruining N, Cho JM, Chowdhary S, Costa MA, de Silva R, Dijkstra J, Di Mario C, Dudek D, Falk E, Feldman MD, Fitzgerald P, Garcia-Garcia HM, Gonzalo N, Granada JF, Guagliumi G, Holm NR, Honda Y, Ikeno F, Kawasaki M, Kochman J, Koltowski L, Kubo T, Kume T, Kyono H, Lam CC, Lamouche G, Lee DP, Leon MB, Maehara A, Manfrini O, Mintz GS, Mizuno K, Morel MA, Nadkarni S, Okura H, Otake H, Pietrasik A, Prati F, Räber L, Radu MD, Rieber J, Riga M, Rollins A, Rosenberg M, Sirbu V, Serruys PW, Shimada K, Shinke T, Shite J, Siegel E, Sonoda S, Suter M, Takarada S, Tanaka A, Terashima M, Thim T, Uemura S, Ughi GJ, van Beusekom HM, van der Steen AF, van Es GA, van Soest G, Virmani R, Waxman S, Weissman NJ, Weisz G, International Working Group for Intravascular Optical Coherence Tomography (IWG-IVOCT) (2012) Consensus standards for acquisition, measurement, and reporting of intravascular optical coherence tomography studies: a report from the International Working Group for Intravascular Optical Coherence Tomography Standardization and Validation. J Am Coll Cardiol 59:1058–1072
17. Lee SY, Shin DH, Mintz GS, Kim JS, Kim BK, Ko YG, Choi D, Jang Y, Hong MK (2013) Optical coherence tomography-based evaluation of in-stent neoatherosclerosis in lesions with more than 50% neointimal cross-sectional area stenosis. EuroIntervention 9:945–951
18. Takano M, Yamamoto M, Inami S, Murakami D, Ohba T, Seino Y, Mizuno K (2009) Appearance of lipid-laden intima and neovascularization after implantation of bare-metal stents extended late-phase observation by intracoronary optical coherence tomography. J Am Coll Cardiol 55:26–32
19. Yonetsu T, Kato K, Kim SJ, Xing L, Jia H, McNulty I, Lee H, Zhang S, Uemura S, Jang Y, Kang SJ, Park SJ, Lee S, Yu B, Kakuta T, Jang IK (2012) Predictors for neoatherosclerosis: a retrospective observational study from the optical coherence tomography registry. Circ Cardiovasc Imaging 5:660–666
20. Yamamoto MH, Yamashita K, Matsumura M, Fujino A, Ishida M, Ebara S, Okabe T, Saito S, Hoshimoto K, Amemiya K, Yakushiji T, Isomura N, Araki H, Obara C, McAndrew T, Ochiai M, Mintz GS, Maehara A (2017) Serial 3-vessel optical coherence tomography and intravascular ultrasound analysis of changing morphologies associated with lesion progression in patients with stable angina pectoris. Circ Cardiovasc Imaging. https://doi.org/10.1161/CIRCIMAGING.117.006347
21. Shimokado A, Matsuo Y, Kubo T, Nishiguchi T, Taruya A, Teraguchi I, Shiono Y, Orii M, Tanimoto T, Yamano T, Ino Y, Hozumi T, Tanaka A, Muragaki Y, Akasaka T (2018) In vivo optical coherence tomography imaging and histopathology of healed coronary plaques. Atherosclerosis 275:35–42
22. Prati F, Romagnoli E, Burzotta F, Limbruno U, Gatto L, La Manna A, Versaci F, Marco V, Di Vito L, Imola F, Paoletti G, Trani C, Tamburino C, Tavazzi L, Mintz GS (2015) Clinical impact of OCT findings during PCI: The CLI-OPCI II study. JACC Cardiovasc Imaging 8:1297–1305
23. Russo M, Fracassi F, Kurihara O, Kim HO, Thondapu V, Araki M, Shinohara H, Sugiyama T, Yamamoto E, Lee H, Vergallo R, Crea F, Biasucci LM, Yonetsu T, Minami Y, Soeda T, Fuster V, Jang IK (2020) Healed plaques in patients with stable angina pectoris. Arterioscler Thromb Vasc Biol 40:1587–1597
24. Amano H, Noike R, Saito D, Yabe T, Watanabe I, Okubo R, Koizumi M, Toda M, Ikeda T (2019) Plaque characteristics and slow flow during percutaneous coronary intervention of irregular protrusion by optical coherence tomography. Heart Vessels 34:1076–1085
25. Park SJ, Kang SJ, Virmani R, Nakano M, Ueda Y (2012) In-stent neoatherosclerosis: a final common pathway of late stent failure. J Am Coll Cardiol 59:2051–2057
26. Kozuki A, Shinke T, Otake H, Shite J, Nakagawa M, Nagoshi R, Hariki H, Inoue T, Osue T, Taniguchi Y, Nishio R, Hirata KI (2013) Temporal course of vessel healing and neoatherosclerosis after DES implantation. JACC Cardiovasc Imaging 6:1121–1123
27. Davies MJ (1994) (1994) Pathology of arterial thrombosis. Br Med Bull 50:789–802
28. Song L, Mintz GS, Yin D, Yamamoto MH, Chin CY, Matsumura M, Fall K, Kirtane AJ, Parikh MA, Moses JW, Ali ZA, Shlofmitz RA, Maehara A (2017) Neoatherosclerosis assessed with optical coherence tomography in restenotic bare metal and first- and second-generation drug-eluting stents. Int J Cardiovasc Imaging 33:1115–1124
29. Otsuka F, Vorpahl M, Nakano M, Foerst J, Newell JB, Sakakura K, Kutys R, Ladich E, Finn AV, Kolodgie FD, Virmani R (2014) Pathology of second-generation everolimus-eluting stents versus first-generation sirolimus- and paclitaxel-eluting stents in humans. Circulation 129:211–223
30. de Goma EM, de Goma RL, Rader DJ (2008) Beyond high-density lipoprotein cholesterol levels: evaluating high-density lipoprotein function as influenced by novel therapeutic approaches. J Am Coll Cardiol 51:2199–2211
31. Eren E, Yilmaz N, Aydin O (2012) High density lipoprotein and it's dysfunction. Open Biochem J 6:78–93
32. Nagano Y, Otake H, Toba T, Kuroda K, Shinkura Y, Tahara N, Tsukiyama Y, Yanaka K, Yamamoto H, Nagasawa A, Onishi H, Sugizaki Y, Takeshige R, Harada A, Murakami K, Kiriyama M, Oshita T, Irino Y, Kawamori H, Ishida T, Toh R, Shinke T, Hirata KI (2019) Impaired cholesterol-uptake capacity of HDL might promote target-lesion revascularization by inducing neoatherosclerosis after stent implantation. J Am Heart Assoc. https://doi.org/10.1161/JAHA.119.011975
33. Deftereos S, Giannopoulos G, Kossyvakis C, Kaoukis A, Raisakis K, Driva M, Panagopoulou V, Lappos S, Rentoukas I, Pyrgakis V, Alpert MA (2010) Effect of quinapril on in-stent restenosis and relation to plasma apoptosis signaling molecules. Am J Cardiol 105:54–58
34. Ohya M, Kadota K, Kubo S, Tada T, Habara S, Shimada T, Amano H, Izawa Y, Hyodo Y, Otsuru S, Hasegawa D, Tanaka H, Fuku Y, Goto T, Mitsudo K (2016) Incidence, predictive factors, and clinical impact of stent recoil in stent fracture lesion after drug-eluting stent implantation. Int J Cardiol 214:123–129
35. Ito T, Kimura M, Ehara M, Terashima M, Nasu K, Kinoshita Y, Habara M, Tsuchikane E, Suzuki T (2014) Impact of sirolimus-eluting stent fractures without early cardiac events on long-term clinical outcomes: a multislice computed tomography study. Eur Radiol 24:1006–1012